Finding Straight Line Generators through the Approximate Synthesis of Symmetric Four-bar Coupler Curves

Aravind Baskar, Mark Plecnik, and Jonathan D. Hauenstein[??]

University of Notre Dame, Notre Dame, IN 46556, USA

Abstract

The approximate path synthesis of four-bar linkages with symmetric coupler curves is presented. This includes the formulation of a polynomial optimization problem, a characterization of the maximum number of critical points, a complete numerical solution by homotopy continuation, and application to the design of straight line generators. Our approach specifies a desired curve and finds several optimal four-bar linkages with a coupler trace that approximates it. The objective posed simultaneously enforces kinematic accuracy, loop closure, and leads to polynomial first order necessary conditions with a structure that remains the same for any desired trace leading to a generalized result. Ground pivot locations are set as chosen parameters, and it is shown that the objective has a maximum of 73 critical points. The theoretical work is applied to the design of straight line paths. Parameter homotopy runs are executed for 1440 different choices of ground pivots for a thorough exploration. These computations found the expected linkages, namely, Watt, Evans, Roberts, Chebyshev, and other previously unreported linkages which are organized into a 2D atlas using the UMAP algorithm.

Key words: Optimization, Homotopy continuation, Straight line generators, Four-bar mechanisms

1. Introduction

The synthesis of a point path by a four-bar linkage has been addressed in [2] for the exact case, and in [3, 4] for the approximate case. Here we address a subcase, that is the synthesis of symmetric coupler curves. A four-bar produces a symmetric coupler only if certain constraints are placed on its dimensions, which have been outlined in [5, 6, 7]. We are motivated to study symmetric curves as we note that many of the special straight line generators found over time produce symmetric curves, e.g., the Watt linkage, the Evans linkage, the Roberts linkage, the Chebyshev linkage, and the Chebyshev lambda linkage [8]. In search of more such interesting geometries, symmetry constraints are installed. This reduces the well known nine dimensional design space of four-bar linkages down to seven dimensions. In addition, to aid in computational tractability, the positions of ground pivots were set, reducing the design space to three dimensions. The relevant kinematic constraints were formulated into an optimization problem which was solved completely for all minima using polynomial homotopy continuation [9]. The result is used to search for straight line generators by systematically varying ground pivot locations and computing several parameter homotopies. Our computational search found the well-known straight line generators as well as several unreported geometries. The resulting linkage designs are organized into an atlas using the UMAP unsupervised manifold learning algorithm [10].

2. Mathematical formulation of four-bars

Consider a planar four-bar linkage as shown in Fig. 1 in the complex plane. Let A and B represent the two fixed pivots, respectively. For representing vector variables such as the fixed pivots, isotropic co-

[1]Corresponding author: Aravind Baskar (abaskar at nd dot edu)

A previous version of the work [1] was presented at the 18th International Symposium on Advances in Robot Kinematics held at Bilbao, Spain, 26-30 June 2022.

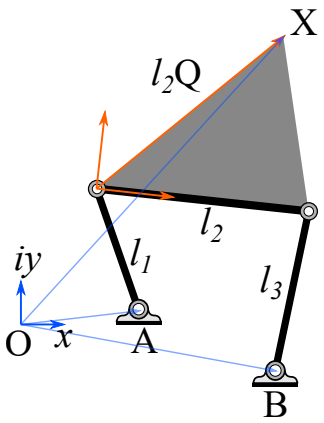

Figure 1: Schematic of a four-bar linkage in the complex plane

ordinates [11] are used here. Hence, additional variables A^* and B^* denoting the conjugate variables of A and B, respectively, are introduced. This is an alternative approach to the Cartesian framework in order to gain certain advantages [11] during the mathematical formulation stage as well as in the implementation of numerical continuation solution technique that follows. Let l_1, l_2, and l_3 be the real variables which denote the lengths of the three moving links as shown. Let ϕ_1, ϕ_2, and ϕ_3 be the respective angular displacements of these links measured counter-clockwise from the positive x-axis. The coupler trace point (normalized by the coupler base length l_2) is represented in the local frame of the coupler as Q and its conjugate counterpart Q^*. In other words, Q is a stretch-rotation that transforms real length l_2 into local complex coordinates of the trace point. The design architecture variables of the four-bar linkage are summarized as $\boldsymbol{d} = \{A, A^*, B, B^*, l_1, l_2, l_3, Q, Q^*\}$. Let X and its conjugate X^* denote the locus of the trace point of interest in the global frame.

We introduce rotation operators in 2D, namely, $\Phi_k = e^{i\phi_k}$ for $k = 1, 2, 3$. The vector loop equations are formulated via the left and right dyads, respectively, as

$$A + l_1\Phi_1 + l_2Q\Phi_2 = X, \tag{1}$$
$$B + l_3\Phi_3 + l_2(Q-1)\Phi_2 = X. \tag{2}$$

The rotation operators are not design specifications for path synthesis applications, hence it is desirable to eliminate them early in the formulation. In order to eliminate them, the complex conjugate equations must also be considered in the isotropic coordinates framework, namely,

$$A^* + l_1\frac{1}{\Phi_1} + l_2Q^*\frac{1}{\Phi_2} = X^*, \tag{3}$$
$$B^* + l_3\frac{1}{\Phi_3} + l_2(Q^*-1)\frac{1}{\Phi_2} = X^*. \tag{4}$$

The conjugate of a rotation operator is its reciprocal from its definition. From Eqns. (1-4), all three rotation operators can be eliminated via polynomial *resultants* sequentially in order to obtain a scalar coupler trace equation $f(X, X^*; \boldsymbol{d}) = 0$ given by:

$$\begin{vmatrix} Q^*(A-X) & g(X,X^*;\boldsymbol{d}) & l_2Q(A^*-X^*) & 0 \\ 0 & l_2Q^*(A-X) & g(X,X^*;\boldsymbol{d}) & Q(A^*-X^*) \\ (Q^*-1)(B-X) & h(X,X^*;\boldsymbol{d}) & l_2(Q-1)(B^*-X^*) & 0 \\ 0 & l_2(Q^*-1)(B-X) & h(X,X^*;\boldsymbol{d}) & (Q-1)(B^*-X^*) \end{vmatrix} = 0, \tag{5}$$

where

$$g(X, X^*; \boldsymbol{d}) = l_2^2QQ^* - l_1^2 + (A-X)(A^*-X^*) \qquad \text{and}$$
$$h(X, X^*; \boldsymbol{d}) = l_2^2(Q-1)(Q^*-1) - l_3^2 + (B-X)(B^*-X^*).$$

As is well known for four-bar linkages, Eq. (5) is a sextic equation with circularity 3. It comprises of 16 distinct monomial terms in X, X^*, namely,

$$\left\{ \begin{array}{l} X^3X^{*3}, X^3X^{*2}, X^3X^*, X^3, X^2X^{*3}, X^2X^{*2}, \\ X^2X^*, X^2, XX^{*3}, XX^{*2}, XX^*, X, X^{*3}, X^{*2}, X^*, 1 \end{array} \right\}$$

in which the coefficient of the leading term X^3X^{*3} is equal to 1. The coefficient expressions are explicitly provided in A for the interested reader.

Four-bar linkages that share an identical coupler locus occur as *Roberts cognate triplets*[2] in the four-bar design space (see [5, pp. 168-176]). For a design $\boldsymbol{d}_1 = \{A, A^*, B, B^*, l_1, l_2, l_3, Q, Q^*\}$, its other two cognates can be expressed as:

$$\begin{aligned} \boldsymbol{d}_2 = \Big\{ & B, B^*, A + Q(B-A), A^* + Q^*(B^*-A^*), l_2\sqrt{(1-Q)(1-Q^*)}\,, \\ & l_3\sqrt{(1-Q)(1-Q^*)}, l_1\sqrt{(1-Q)(1-Q^*)}, \frac{1}{1-Q}, \frac{1}{1-Q^*} \Big\}, \\ \boldsymbol{d}_3 = \Big\{ & A + Q(B-A), A^* + Q^*(B^*-A^*), A, A^*, l_3\sqrt{QQ^*}, \\ & l_1\sqrt{QQ^*}, l_2\sqrt{QQ^*}, \frac{Q-1}{Q}, \frac{Q^*-1}{Q^*} \Big\}. \end{aligned} \tag{6}$$

In our computational experiment, we restrict the model to four-bars that generate symmetric coupler curves. We do this for two reasons. First, much of the straight line linkages reported in the literature [8] such as Watt, Evans, Roberts, and Chebyshev linkages generate symmetric coupler curves about some axis of symmetry in the plane. Second, the inclusion of additional conditions on the design variables to this effect simplifies the model significantly and enables faster computations.

2.1. Symmetric coupler curves

The following derives the necessary and sufficient conditions for a four-bar linkage to generate symmetric coupler curves. While some of these conditions can be found in the literature, we present a direct proof here via analytical geometry and symbolic algebraic analysis.

Since we are working with isotropic coordinates, the first step is to derive the equation of axis of symmetry in isotropic coordinates. Following the isotropic coordinates convention $P = p + iq$, where i is the imaginary unity, points (P, P^*) on a generic line (axis of symmetry) in the complex plane satisfy:

$$L(P, P^*) = K^*P + KP^* + c = 0. \tag{7}$$

Note that K denotes any vector represented in isotropic coordinates along the normal to the axis of symmetry, and c is a real parameter such that $c = -K^*D - KD^*$ for any point D on the symmetric axis. If (X, X^*) is any point in the plane, then its symmetric reflection about the axis given by Eq. (7) is

$$(X_m, X_m^*) = \left(-\frac{c + KX^*}{K^*}, -\frac{c + K^*X}{K} \right). \tag{8}$$

It follows that for a four-bar coupler curve to be symmetric about an axis $L(P, P^*) = 0$, (X_m, X_m^*) given by Eq. (8) must also satisfy Eq. (5), that is, $f(X_m, X_m^*; \boldsymbol{d}) = 0$. This equation must be a constant multiple of the original four-bar coupler curve, $f(X, X^*; \boldsymbol{d}) = 0$ for a four-bar linkage to generate a symmetric coupler curve about any axis in plane. Hence,

$$f(X_m, X_m^*; \boldsymbol{d}) = \lambda f(X, X^*; \boldsymbol{d}), \tag{9}$$

where $\lambda = \frac{1}{K^3K^{*3}}$ is a constant that balances the leading term X^3X^{*3} on both sides. This constant arises due to the presence of K and K^* in the denominator terms of X_m^* and X_m, respectively, in Eq. (8). Subsequently,

[2]These are different from Roberts straight line linkage which is a specific four-bar linkage attributed to the same person.

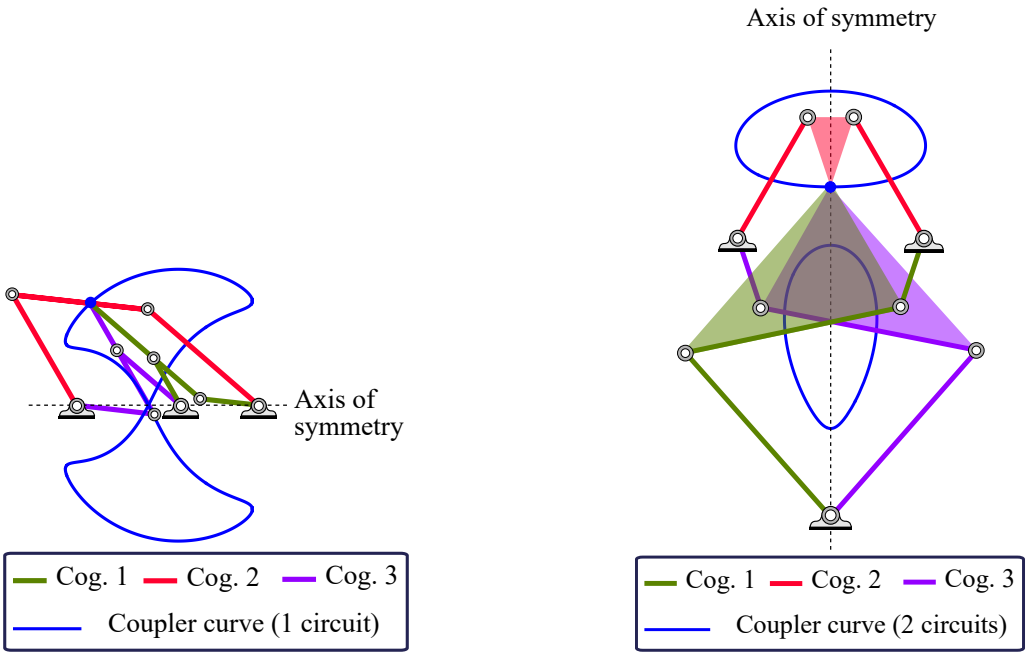

(a) Class A (b) Class B

Figure 2: Two classes of four-bar linkages which generate symmetric coupler curves

the coefficients of the 16 monomial terms in X, X^* can be equated element-wise for consistency to arrive at 15 conditions (disregarding the leading term X^3X^{*3}) on the design variables $\boldsymbol{d}$ and the axis parameters K, K^*, c. As the symmetric behavior is unaffected by scaling, rotation, and translation, the fixed pivots can be chosen as $A = A^* = 0$ and $B = B^* = 1$ which further simplifies the conditions. Note that this choice of fixed pivots is made only for enabling the derivation of the conditions of symmetry and is not a global choice for the latter sections on numerical results.

Of the 15 consistency conditions, the conditions corresponding to the monomials X^3, X^3X^*, X^3X^{*2} are the easiest to manipulate algebraically. These are described, respectively, as follows:

$$c\,(c+K)\,(c+KQ^*) = 0. \tag{10}$$

$$-3c^2 - 2cK^* - 2cK^*Q - K^{*2}Q + K^2Q^* = 0, \tag{11}$$

$$3c + K + K^* + K^*Q + KQ^* = 0, \tag{12}$$

The conjugate of these conditions also occur corresponding to the monomials $X^{*3}, XX^{*3}, X^2X^{*3}$. Note that these three conditions and their conjugate counterparts are only dependent on c, K, K^*, Q and Q^*.

Equation (10) shows that either $c = 0$, $c = -K$, or $c = -KQ^*$. In the following, these three conditional branches are analyzed separately with Eqs. (11,12), and then with the other 12 coefficient conditions, which are not all independent.

2.1.1. Case 1: $c = 0$

If $c = 0$, Eqs. (11,12) simplify into the following, respectively:

$$-K^{*2}Q + K^2Q^* = 0, \tag{13}$$

$$K + K^* + K^*Q + KQ^* = 0. \tag{14}$$

This system of two linear equations in Q, Q^* further bifurcates into the following cases depending on whether the system is rank-deficient or well-determined.

- If the above system is rank-deficient, then the consistency conditions are $K = -K^*, Q = Q^*$ along with $c = 0$. We note that for these conditions, all the 15 consistency conditions given by Eq. (9) vanish.

Upon interpretation of these conditions geometrically, these correspond to four-bars whose trace point lie along the line connecting the two floating pivots as shown in Fig. 2a, termed **Class A** linkages. The reflections of these linkages about their ground link in any given configuration are also part of their configuration space, thus enabling the occurrence of symmetric coupler curves. The cognates of such four-bars also meet these conditions with the ground-pivots of all three cognates lying along the axis of symmetry.

- On the other hand, if the system is well-determined, then the variables Q and Q^* can be solved as: $Q = -\frac{K}{K^*}, Q^* = -\frac{K^*}{K}$. Under these, all the other conditions given by Eq. (9) are met only when $l_1 = l_2$. These linkages are termed as **Class B** linkages. To be more precise, these conditions correspond to one of the three Roberts cognate sub-classes of Class B, as will be made evident from subsequent derivations.

2.1.2. Case 2: $c = -K = -K^*$

In this case, Eqs. (11,12) are consistent if and only if $Q^* = 1 - Q$. Further analysis of Eq. (9) shows that $l_1 = l_3$ must also hold for all the conditions to be met. These linkages are the Roberts cognates of the Class B linkages in the earlier step. An example of a linkage that meets these conditions is shown as cognate #2 in Fig. 2b.

2.1.3. Case 3: $c = -KQ^* = -K^*Q$

Upon similar analysis, it can be shown that the consistency conditions are $Q^* = \frac{Q}{Q-1}$ and $l_2 = l_3$. As expected, these are the third Roberts cognates of Class B.

2.2. Summary of four-bar linkages that generate symmetric coupler curves

Four-bar linkages that generate coupler curves symmetric about an axis in the plane are of the following two classes:
Class A: $Q = Q^*$. These four-bars generate symmetric coupler curves only due to the special choice of trace point along its coupler base, leading to a mirror symmetry of the coupler curves about their respective ground links. This class of four-bars does not require any special conditions on the link lengths l_1, l_2 and l_3. The cognates of such four-bars also adhere to the same conditions.
Class B: The other class of four-bars generating symmetric coupler curves can be split into three sub-classes which constitute a Roberts cognate triplet.

1. $Q = \frac{1}{Q^*}, l_1 = l_2$
2. $Q^* = 1 - Q, l_1 = l_3$
3. $Q^* = \frac{Q}{Q-1}, l_2 = l_3$

Arguably, four-bars of Class B are more interesting because, unlike Class A, the symmetric curves generated by them are not mere reflections about the axis defined by their respective ground links. The axis of symmetry in the four-bars of Class B is the perpendicular bisector of the fixed link corresponding to cognate #2. It also passes through the ground pivot shared between the cognates #1 and #3 as shown in Fig. 2b. For further description of the four-bars of Class B and their geometry, refer to [5, 7]. Roberts linkage is a well-known symmetric straight line linkage, which is of Class B. The two classes of four-bars can also overlap in the design space with two mutually perpendicular axes of symmetry in their coupler curves as exhibited in some notable cases in literature such as Evans, Chebyshev and Watt straight line linkages, see Fig. 3.

In the following, we generate an atlas of straight line generating four-bar mechanisms using an optimization approach based in polynomial homotopy continuation. We limit the investigation to the four-bars of Class B. Our initial investigation into Class A four-bars were underwhelming for this application as the best straight line generating four-bars of Class A appear to also belong to Class B as shown in Fig. 3. Hence, we solve for cognate #2 of Class B and compute cognates #1 and #3 based on the transformations presented in Eq. (6).

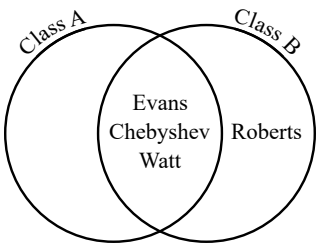

Figure 3: Categorization of Evans, Chebyshev, Watt, and Roberts straight line linkages as either Class A or Class B symmetric four-bars.

3. Optimization model for approximating desired curves using symmetric four-bar coupler curves

A generic four-bar design is represented as $\boldsymbol{d} = \{A, A^*, B, B^*, l_1, l_2, l_3, Q, Q^*\}$ by our earlier convention. Note that $l_1 = l_3 = l$ and $Q^* = 1 - Q$ based on the architecture conditions derived for cognate #2 of Class B. This simplifies the coupler equation in terms of $\{A, A^*, B, B^*, l, l_2, Q\}$. Further, since $Q + Q^* = 1$, the variable Q can be represented using $\frac{1}{2} + iq_y$, where q_y is a real variable and i the imaginary unit. As the variables l and l_2 occur only in the form of squares, modified real variables $l_{2s} = l_2^2$ and $l_s = l^2 - \frac{l_{2s}}{4}(1 + 4q_y^2)$ are introduced based on careful observation of the polynomial structure to simplify the equation further and to reduce the total degree. At this stage, a decision is made to treat A, A^*, B, B^* as specified design parameters instead of treating them as variables. This brings down the number of variables, all real, to 3, namely, l_s, l_{2s} and q_y, as opposed to being 7 which would be a more difficult problem outside the scope of this work.

As mentioned earlier, the coupler curve of a four-bar linkage is degree six. Hence, if the exact synthesis approach is taken, a maximum of only six design positions along a straight line can be specified. Approximate synthesis process allows for as many design specifications as desired. The optimization problem is one of minimizing the error residue of the coupler equation over all the design positions. We chose the $\boldsymbol{L}^2$-norm to retain the polynomial nature of the objective function, thus allowing the use of a polynomial homotopy continuation approach to solve any resulting polynomial system.

The objective of the optimization problem is a sum of squares of the residue of the coupler equation over all the design positions, $j = 1, 2, ..., N$:

$$\sum_{j=1}^{N} \eta_j^2, \tag{15}$$

where $\eta_j = f(X_j, X_j^*; A, A^*, B, B^*, l_s, l_{2s}, q_y)$. The design positions are X_j, X_j^*, the design parameters are A, A^*, B, B^*, the design variables are l_s, l_{2s}, q_y, and the number N can be arbitrarily large. As N increases to infinity, if the desired curve segment can be represented in a continuous parametric form, say $X(t), X^*(t)$ for $t \in [t_i, t_f]$, then the objective function can also be written as a definite integral:

$$\xi = \int_{t_i}^{t_f} \eta^2 dt. \tag{16}$$

The integrand is a polynomial in the design variables l_s, l_{2s}, q_y of 55 distinct monomials including the unit monomial 1. The coefficients of these monomials are parametric functions of $A, A^*, B, B^*, X(t), X^*(t)$ and can be integrated with respect to t to obtain numerical values. Hence, one can view these numerical values as functions of A, A^*, B, B^* and moments of the curve, which is a generalization of moments of continuous random variables e.g., see [12, Chap. 4]. In particular, the 49 moments of the curve arising are $M_{j,k}$ for $0 \leq j, k \leq 6$ where

$$M_{j,k} = \int_{t_i}^{t_f} X(t)^j X^*(t)^k dt.$$

Irrespective of the desired curve, the optimization objective is of a certain polynomial structure with 55 linear coefficient parameters thereby presenting a unified framework to solve path synthesis problems of this kind.

The first-order necessary conditions of optimality are then derived symbolically as:

$$\begin{pmatrix} \frac{\partial \xi}{\partial l_s} \\ \frac{\partial \xi}{\partial l_{2s}} \\ \frac{\partial \xi}{\partial q_y} \end{pmatrix} = \mathbf{0}. \tag{17}$$

This system of 3 equations in 3 unknowns has a polynomial structure that is invariant to the desired curve being specified following the same reasoning as before. In particular, the total degree of this polynomial system is 648, which forms a trivial upper bound of the number of critical points of the objective function. One can compute tighter bounds such as a 2-homogeneous Bézout bound [11] of 186 and the BKK bound [11] of 73. This is confirmed by explicitly solving a randomly chosen *ab initio* system using the numerical continuation solver `Bertini` [9, 13] via a 2-homogeneous homotopy of 186 startpoints. Such a start system is usually constructed by forming a polynomial system respecting the same multi-homogeneous structure using linear expressions which are easily solved to form the startpoints [2, 14]. Then, using a predictor-corrector numerical path tracking, the startpoints are deformed continuously to the target points of the ab initio system. Solving this *ab initio* system yielded 73 solutions matching the BKK bound, while the rest diverged off to infinity as expected. Thus, one can use a parameter homotopy [9] and track 73 solution paths to solve any other system with this polynomial structure.

4. Design of experiments for approximating a straight line segment

Parameter homotopy runs are carried out for the design of approximate straight line generating four-bar linkages with cognate #2 symmetric four-bars of Class B being the primary focus. The design specification is chosen as a unit segment along the x-axis in the range $[-0.5, 0.5]$. This can be written in the parametric form $X(t) = X^*(t) = t, t \in [-0.5, 0.5]$. In order to explore the design space, the locations of ground pivots, which appear in our formulation as specifications, were systematically varied. The ground link is described by four parameters, two for each fixed pivot. We add a constraint that restricts the ground link such that the axis of symmetry passing through either the mid-point, referred as Specification I, or at the end of the desired segment, referred as Specification II, as shown in Fig. 4a and 4b, respectively, parameterized via r, θ, and s as illustrated. These two specifications types lead to noticeably different four-bar linkage designs because of the relative positioning of the symmetric axis vis-à-vis the specified line segment. The parameter θ was restricted to be within $[0°, 90°]$ in the case of Specification I and $[0°, 180°]$ in the case of Specification II

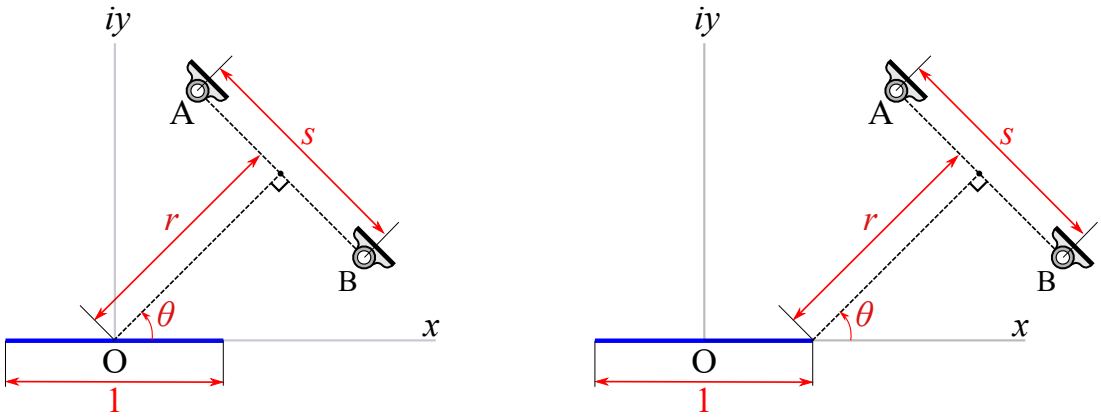

(a) Specification I (b) Specification II

Figure 4: Design specification for approximate straight line generating four-bar linkages. In both the scenarios, the line segment is of the parametric form $X(t) = X^*(t) = t, t \in [-0.5, 0.5]$. In the first scenario, the axis of symmetry passes through the mid-point of the desired segment while in the second, it passes through the end.

as extending these ranges any further leads to mirror specifications. We sample the space by employing a discretization scheme as follows:

$$\text{Specification I:} \quad r \in \{0.25i\}_{i=0}^{8} \qquad \theta \in \{15^\circ j\}_{j=0}^{6} \qquad s \in \{0.25k\}_{k=1}^{8}, \tag{18}$$

$$\text{Specification II:} \quad r \in \{0.25i\}_{i=0}^{8} \qquad \theta \in \{15^\circ j\}_{j=0}^{1} 2 \qquad s \in \{0.25k\}_{k=1}^{8}, \tag{19}$$

which yields a total of $9 \cdot 7 \cdot 8 = 504$ problems for Specification I and $9 \cdot 13 \cdot 8 = 936$ for Specification II, respectively, totalling[3] 1440.

The computation time required for solving a single parameter homotopy run of 73 paths is about 15s on average. Most of these runs were 100% successful with 73 endpoints. For some special parameter sets such as when $r = 0$ and/or $\theta = 0^\circ, 90^\circ$ or 180°, some of the 73 paths, diverged to infinity. This can be explained by the special nature of these parameters which can result in certain monomials vanishing to zero identically. Among the successful endpoints of the parameter homotopy runs, only the solutions that correspond to physical linkages are retained and the rest are discarded. The physical linkages include local minima as well as saddle points of the respective optimization objective. From prior experience in solving optimization problems in mechanism synthesis [15], some saddle points have been known to meet the design requirements quite well. Thus, at this stage all physical linkages are retained irrespective of whether they correspond to minima or saddle points. Consolidating the physical solutions resulting from all 1440 parameter homotopy runs yields 16,904 linkages. This set is then further pruned based on an allowable structural error tolerance of $\frac{1}{100}$ of unity in the y direction of the desired segment. This results in 190 linkages of which cognates #1 and #3 are computed based on Eq. (6), totalling $3 \cdot 190 = 570$. A further rejection of linkages with any link length greater than 2 resulted in 274 distinct approximate straight line generating four-bars.

For exhibiting these 274 linkages, we used the manifold learning technique UMAP [10], a nonlinear dimensional reduction tool to allow us to visualize higher dimensional data in 2D. Using the ground-pivots and the link dimensions to represent each four-bar linkage and setting the hyper-parameters of UMAP, namely, `min_dist=0.05` and `n_neighbors=10`, Fig. 5 is produced as a lower dimensional embedding. It shows bunches of coupler curves which are organized into bins, colored and labelled distinctly, by inspection based on the results of UMAP. The coupler curves within each bin are plotted on the same axis to scale. Some of these coupler curves correspond to popular straight line generating four-bars such as Watt, Evans, Roberts and Chebyshev linkages and their cognates. Additionally, we found a lot of variants of these popular linkages as well as other previously unreported linkages as shown in Fig. 6 with representative examples colored and labelled according to the bin to which they belong in Fig. 5. Our computational approach produced hundreds of linkages that serve as a useful atlas for designers[4].

5. Conclusion

In this paper, the synthesis equations were formulated, characterized, and solved for a four-bar linkage with ground pivots specified to produce a desired symmetric coupler curve approximately. The solution is applied to search for four-bar approximate straight line generators by solving an optimization problem. The mathematical model is restricted to one particular class of four-bars which generate symmetric coupler curves to reduce the computational challenges associated with solving a generic four-bar linkage system. The validity of our approach is affirmed by rediscovering the classical approximate straight line generators by solving an easier system. In addition, we found more approximate straight line generators which are substantially different from the classical linkages. Using the UMAP algorithm, our results are organized into a 2D atlas, which could be a useful reference for mechanical designers in need of more straight line options.

Acknowledgement

This material was supported by the National Science Foundation under Grant No. CMMI-2041789. The last author appreciates the comments provided by the audience of the Algebraic Geometry and Machine Learning Mini-Symposium at the 2022 SIAM Conference on Mathematics of Data Science about this work.

[3] A tiny fraction of these are not distinct problems and they occur in both the Specifications.

[4] Refer to DOI: 10.7274/bg257d30h7p for Supplementary Wolfram Mathematica [16] files exhibiting all 274 linkages.

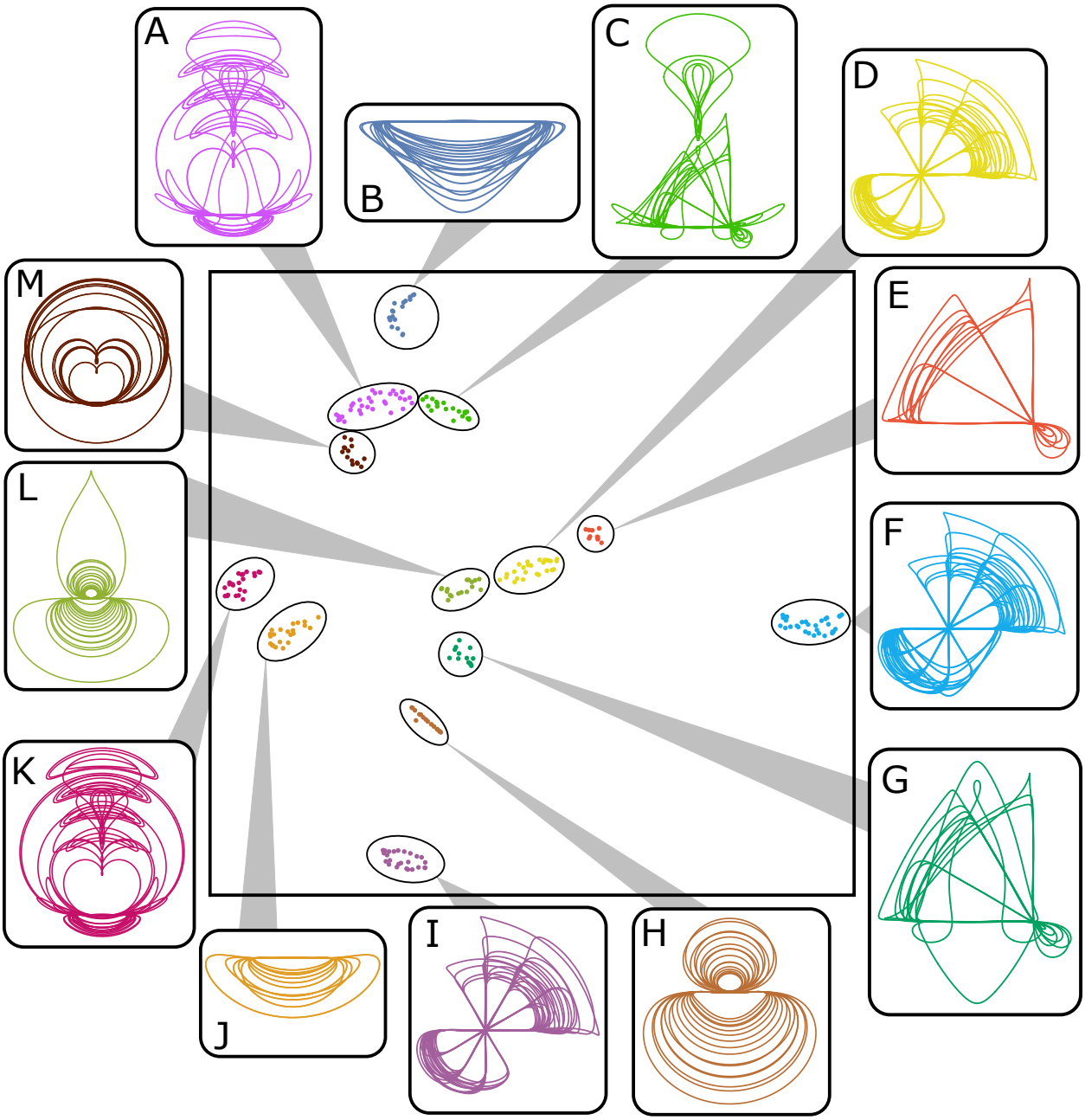

Figure 5: An atlas of four-bar coupler curves that generate an approximate straight line segment visualized using UMAP.

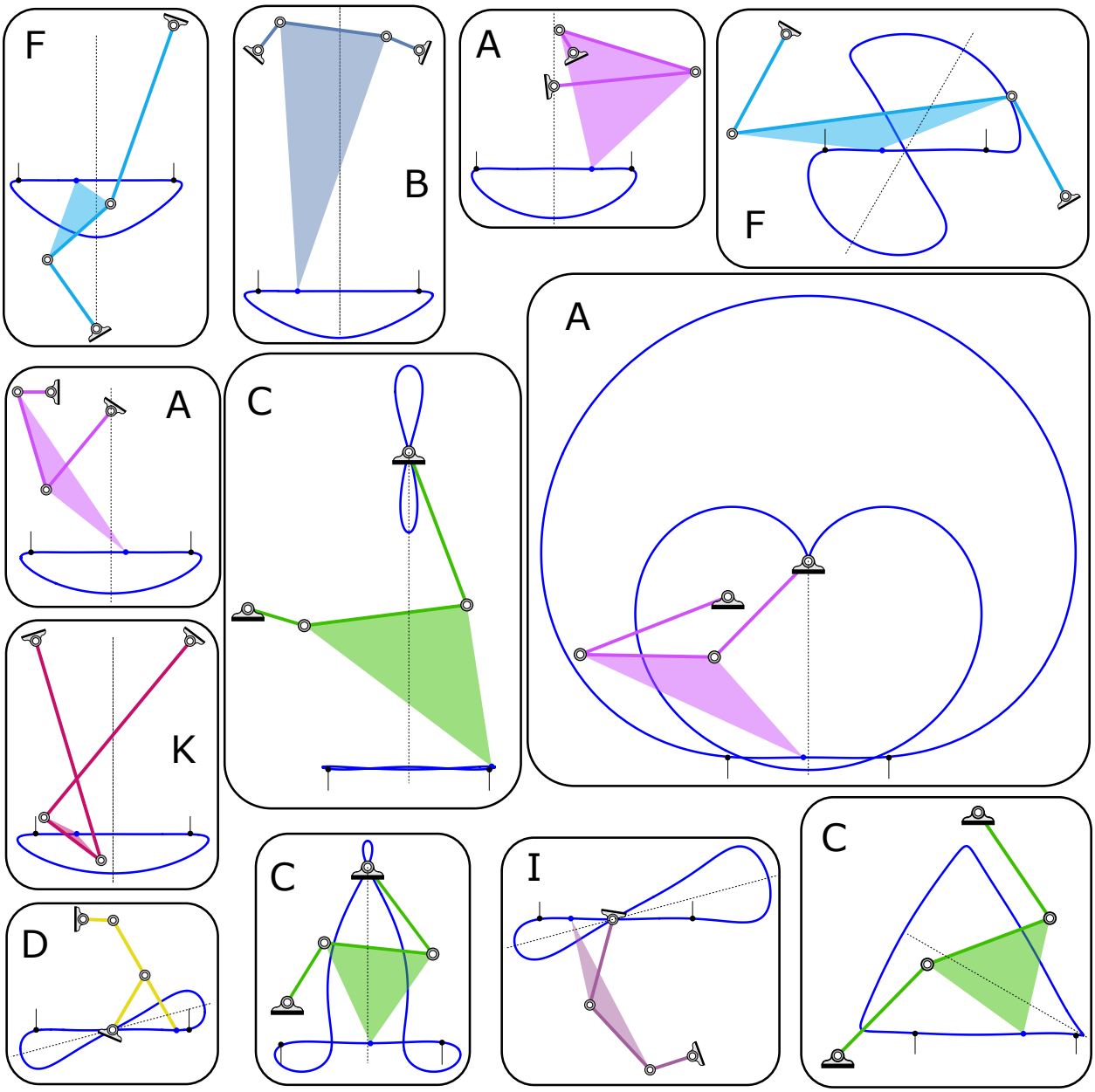

Figure 6: A representative collection of straight line generating four-bar linkages found by numerical continuation enabled optimization. All the linkages are shown to the same scale with the approximate straight line segment marked by pointers at its extremities and the axis of symmetry by a dashed line.

A. Four-bar coupler trace equation

The following are the monomial terms in X, X^* and their corresponding coefficient expressions in Eq. (5).

$$
\begin{aligned}
X^3X^{*3} &: 1\\
X^3X^{*2} &: A^*(-2+Q^*) - B^*(1+Q^*)\\
X^3X^* &: 2A^*B^* - A^{*2}(-1+Q^*) + B^{*2}Q^*\\
X^3 &: A^*B^*(A^*(-1+Q^*) - B^*Q^*)\\
X^2X^{*2} &: BB^* - 2l_1^2 + BB^*Q + l_1^2Q + l_2^2Q - l_3^2Q - A^*B(1+Q)(-2+Q^*) + (l_1^2 + l_2^2 - l_3^2 - 2l_2^2Q\\
&\quad + BB^*(1+Q))Q^* + A(-2+Q)(A^*(-2+Q^*) - B^*(1+Q^*))\\
X^2X^* &: A^{*2}B(1+Q)(-1+Q^*) - A(-2+Q)(-2A^*B^* + A^{*2}(-1+Q^*) - B^{*2}Q^*)\\
&\quad - A^*(2(l_2-l_3)(l_2+l_3)Q + 2BB^*(1+Q) - l_1^2(-2+Q)(-1+Q^*) + l_2^2(1-4Q)Q^* + l_3^2(-1+Q)Q^*\\
&\quad + l_2^2(-1+2Q)Q^{*2}) - B^*(l_1^2(-2+Q+QQ^*) + Q^*(BB^*(1+Q) - l_3^2(1+Q) + l_2^2(1+Q^*-2QQ^*)))\\
X^2 &: A^{*2}(-(BB^*(1+Q)) + Q(l_3^2 + l_2^2(-1+Q^*)))(-1+Q^*) + AA^*B^*(-2+Q)(A^*(-1+Q^*) - B^*Q^*)\\
&\quad + B^{*2}(-1+Q)Q^*(l_1^2 - l_2^2Q^*) + A^*B^*(-(l_1^2(-2+Q)(-1+Q^*)) + (BB^*(1+Q) - l_3^2(1+Q)\\
&\quad - l_2^2(-1+Q^*))Q^*)\\
XX^* &: l_1^2(-2BB^* - l_1^2(-1+Q) + (l_3^2 + l_2^2(-1+Q))Q) + 2A^*B(Q(BB^* - l_3^2 + l_2^2(-1+Q(-1+Q^*))(-1+Q^*))\\
&\quad + l_1^2(-1+Q^*)) - A^{*2}B^2Q(-1+Q^*) + (B^2B^{*2}Q + (l_1^2 + l_2^2 - l_3^2)(l_1^2(-1+Q) + 2BB^*Q - (l_3^2\\
&\quad + l_2^2(-1+Q))Q))Q^* + l_2^2(-(l_1^2(-1+Q)) + Q(l_3^2 + l_2^2(-1+Q) - 2BB^*Q))Q^{*2} + A^2(-1+Q)\\
&\quad (-2A^*B^* + A^{*2}(-1+Q^*) - B^{*2}Q^*) + 2A(2A^*BB^* + B^*l_1^2(-1+Q) - A^*(-l_3^2 + l_2^2(-1+Q)(-1+Q^*))\\
&\quad (Q(-1+Q^*) - Q^*) + A^{*2}(B - BQ^*) + A^*l_1^2(-1+Q+Q^* - QQ^*) + B^*Q^*(BB^* - l_3^2 + l_2^2(-1+Q)\\
&\quad (-1+(-1+Q)Q^*)))\\
X &: A^{*2}BQ(BB^* - l_3^2 - l_2^2(1+Q)(-1+Q^*))(-1+Q^*) - A^2A^*B^*(-1+Q)(A^*(-1+Q^*) - B^*Q^*)\\
&\quad + B^*(-1+Q)(-l_1^2 + l_2^2QQ^*)(l_1^2(-1+Q^*) + BB^*Q^* - (l_3^2 + l_2^2(-1+Q^*))Q^*) + A^*(-(B^2B^{*2}QQ^*)\\
&\quad + Q(-l_3^2 + l_2^2(-1+Q)(-1+Q^*))(-(l_1^2(-1+Q^*)) + (l_3^2 + l_2^2(-1+Q^*))Q^*) + 2BB^*(-(l_1^2(-1+Q^*))\\
&\quad + Q(l_3^2 + l_2^2(-1+Q^*))Q^*)) + A(A^{*2}(2BB^* - l_3^2Q + l_2^2(-1+Q)Q(-1+Q^*))(-1+Q^*) - B^{*2}(-1+Q)\\
&\quad Q^*(l_1^2 + l_2^2(-2+Q)Q^*) + 2A^*B^*(l_1^2(-1+Q)(-1+Q^*) + Q^*(-(BB^*) + l_3^2 + l_2^2(-1+Q+Q^*-QQ^*))))\\
1 &: A^2B^*(-1+Q)(A^{*2}B(-1+Q^*) + B^*l_2^2(-1+Q)Q^{*2} + A^*Q^*(-(BB^*) + l_3^2 + l_2^2(-1+Q+Q^*-QQ^*)))\\
&\quad + B(-1+Q^*)(B^*(l_1^2 - l_2^2QQ^*)(A^*BQ + (-1+Q)(l_1^2 - l_2^2QQ^*)) + A^*Q(l_1^2(-l_3^2 + l_2^2(-1+Q)(-1+Q^*))\\
&\quad + l_2^2Q(A^*B(-1+Q^*) + Q^*(l_3^2 + l_2^2(-1+Q+Q^*-QQ^*))))) + A(-(A^{*2}BQ(BB^* - l_3^2 + l_2^2(-1+Q)\\
&\quad (-1+Q^*))(-1+Q^*)) + B^*(-1+Q)(BB^* - l_3^2 + l_2^2(-1+Q)(-1+Q^*))Q^*(l_1^2 - l_2^2QQ^*)\\
&\quad + A^*(B^2B^{*2}QQ^* + QQ^*(l_3^2 + l_2^2(-1+Q+Q^*-QQ^*))^2 - 2BB^*(l_1^2(-1+Q)(-1+Q^*)\\
&\quad + QQ^*(l_3^2 + l_2^2(-1+Q+Q^*-QQ^*)))))
\end{aligned}
$$

The coefficients for the remaining monomials, namely, $X^2X^{*3}, XX^{*3}, XX^{*2}, X^{*3}, X^{*2}, X^*$, are simply complex conjugates of the coefficients of their conjugate monomials.

References

[1] A. Baskar, M. Plecnik, J. D. Hauenstein, Finding straight line generators through the approximate synthesis of symmetric four-bar coupler curves, in: International Symposium on Advances in Robot Kinematics, Springer, 2022, pp. 277–285.

[2] C. Wampler, A. Morgan, A. Sommese, Complete solution of the nine-point path synthesis problem for four-bar linkages, Journal of Mechanical Design 114 (1) (1992) 153–159.

[3] F. T. S. Marín, A. P. González, Global optimization in path synthesis based on design space reduction, Mechanism and machine theory 38 (6) (2003) 579–594.

[4] A. Baskar, C. Hills, M. Plecnik, J. D. Hauenstein, Estimating the complete solution set of the approximate path synthesis problem for four-bar linkages using random monodromy loops, ASME International Design Engineering Technical Conferences & Computers and Information in Engineering Conference, American Society of Mechanical Engineers, 2022, pp. IDETC2022–90402.

[5] R. Hartenberg, J. Denavit, Kinematic synthesis of linkages, New York: McGraw-Hill, 1964.

[6] D.-M. Lu, W.-M. Hwang, Spherical four-bar linkages with symmetrical coupler-curves, Mechanism and Machine Theory 31 (1) (1996) 1–10.

[7] A. K. Natesan, Kinematic analysis and synthesis of four-bar mechanisms for straight line coupler curves, Ph.D. thesis, Rochester Institute of Technology (1994).

[8] H. Nolle, Linkage coupler curve synthesis: A historical review—I. developments up to 1875, Mechanism and Machine Theory 9 (2) (1974) 147–168.

[9] D. J. Bates, J. D. Hauenstein, A. J. Sommese, C. W. Wampler, Numerically solving polynomial systems with Bertini, SIAM, Philadelphia, 2013.

[10] L. McInnes, J. Healy, J. Melville, UMAP: Uniform manifold approximation and projection for dimension reduction, arXiv preprint arXiv:1802.03426 (2018).

[11] C. W. Wampler, Isotropic Coordinates, Circularity, and Bezout Numbers: Planar Kinematics From a New Perspective, Vol. 2A: 24th Biennial Mechanisms Conference of International Design Engineering Technical Conferences and Computers and Information in Engineering Conference, 1996, v02AT02A073.

[12] G. R. Grimmett, D. R. Stirzaker, Probability and random processes, 3rd Edition, Oxford University Press, New York, 2001.

[13] D. J. Bates, J. D. Hauenstein, A. J. Sommese, C. W. Wampler, Bertini: Software for numerical algebraic geometry.

[14] A. Morgan, A. Sommese, A homotopy for solving general polynomial systems that respects m-homogeneous structures, Applied Mathematics and Computation 24 (2) (1987) 101–113.

[15] A. Baskar, M. Plecnik, J. D. Hauenstein, Computing saddle graphs via homotopy continuation for the approximate synthesis of mechanisms, Mechanism and Machine Theory 176 (2022) 104932.

[16] Wolfram Research Inc., Mathematica, Version 12.1.0.0, Champaign, IL, 2021.